DISPERSION STUDY OF PROPAGATION OF TORSIONAL SURFACE WAVE IN A LAYERED STRUCTURE

S. Gupta **N. Bhengra***

Department of Applied Mathematics
Indian Institute of Technology (ISM)
Dhanbad, India

ABSTRACT

This paper presents the feasibility of torsional surface wave propagation in an anisotropic layer sandwiched between two anisotropic inhomogeneous media. The anisotropy considered in the upper layer and the lower half-space is of transversely isotropic kind while the sandwiched anisotropic layer is a porous layer. The directional rigidities and density have been considered linearly and exponentially varying in the half-space and in the upper layer respectively, while it is taken as a variable in the sandwiched layer. The compact form of dispersion equation governing the propagation of the torsional surface wave has been derived by using the Whittaker function under appropriate boundary conditions. The dispersion of the torsional wave and the effects of inhomogeneity parameters, initial stress and poroelastic constant have been calculated numerically and demonstrated through graphs.

Keywords: Torsional surface wave, Transversely isotropic medium, Porous medium, Whittaker function.

1. INTRODUCTION

In the present context, a considerable interest has been generated on the study of wave propagation through every type of medium. Mediums such as naturally occurring medium, medium made of man-made materials and complex media, which have widespread application in acoustic signal transmission, seismic exploration, non-destructive evaluation, subsurface exploration, etc. The earth is a layered structural medium under high initial stress and the stresses are jointly produced by the atmospheric pressure, difference in temperature, sedimentation of rocks, thus increasing the overburden pressure. This overburden pressure creates a state of compression in the subsurface environment and gradually the layers become stressed. These may affect the propagation of the seismic waves through the medium and provide valuable information about the configuration and setting of the elastic media for geophysical prospecting. Comprehensive information regarding seismic waves can be gathered from Ewing *et al.* [1], Gubbins [2], and Udias [3] etc.

The study of the torsional surface wave through different anisotropic media became the topic of special interest among the seismologists due to its fascinating behavior. This behavior is justified by the fact that the polarization of the waves are horizontal yet it gives a twist to the medium during propagation. In addition, there is an exponential decay in the amplitude of the torsional surface wave with distance from the free surface. The study of torsional surface wave propagation in different mediums under various circumstances became the open door to many mysterious things, some of the eminent works were presented by Dey and Sarkar [4], Selim [5], Ozturk and Akbarov [6] and Akbarov *et al.* [7] and Chattopadhyay *et al.* [8] etc.

The study of surface wave propagation through fluid saturated media has garnered a lot of recognition from the seismologists, rock engineers, and civil engineers. The classical theory, which considers a fluid saturated porous medium as a single-phase material, is insufficient to explain the mechanical behavior of multiphase porous materials (especially if the pores are filled with fluids). Biot [9-11] formulated the governing equations for fluid-saturated porous media. Biot's equation of linear theory of poroelasticity can be ascribed to a complete general description of the mechanical behavior of a poroelastic medium. Deresiewicz [12-14] derived the dispersion equation for the Love wave propagation in a porous solid first. However, no dispersion and attenuation curves were stated in these papers. Sharma and Gogna [15] discussed the Love waves in an initially stressed medium consisting of an elastic layer overlying a liquid saturated porous half-space with small porosity; on the other hand, attenuation was ignored. Wang and Zhang [16] investigated the Love wave propagation in a

* Corresponding author (neelima.ism@gmail.com)

DOI : 10.1017/jmech.2017.1
Copyright © 2017 The Society of Theoretical and Applied Mechanics
https://doi.org/10.1017/jmech.2017.1 Published online by Cambridge University Press

transversely isotropic fluid saturated porous half-space. Gupta and Gupta [17] developed the study of torsional surface wave propagation in gravitating anisotropic porous half-space. Ke *et al.* [18] discussed the propagation of Love wave in a linearly varying inhomogeneous fluid saturated porous layered half-space.

The crustal layer of earth is composed of various heterogeneous layers with different geological parameters and settings, which makes this study of wave propagation much more practical. There are different types of heterogeneities existing in the crustal layers in the form of hyperbolic, harmonic, exponential, linear, quadratic, etc., for simulating the variation in rigidity, density and other geological parameters inside the earth. Bullen [19] pointed out that the density inside the earth differs at different rates with different layers within the earth. Gupta *et al*. [20] studied the propagation of torsional wave in an initially stressed inhomogeneous elastic layer with a hyperbolic variation and half-space with polynomial variation of shear modulus and density of the medium. Sari and Salk [21] took the hyperbolic function as the variation in the density of sediments.

This problem examines the propagation of the torsional surface wave in double layers of finite width, lying over a half-space, having variation in directional rigidities and densities in the medium. In the present study, the heterogeneity taken is produced by a variation in directional rigidities and density in the medium. The compact form of dispersion equation is obtained which is in well agreement with the classical Love Wave equation. Particular cases have been derived and the obtained results are demonstrated by a graphs.

2. FORMULATION OF THE PROBLEM

Consider a cylindrical coordinate system (r, θ, z) to study the torsional surface wave propagation in a layered structure consisting of an anisotropic porous layer of thickness h_1 sandwiched between an inhomogeneous anisotropic layer of thickness h_2 and an initially stressed inhomogeneous anisotropic half-space. The z–axis is taken vertically downward and r–axis is chosen in the direction of wave propagation. The origin O has been taken at the interface between anisotropic porous layer and inhomogeneous anisotropic half-space, as given in Fig. 1.

In the present paper, variations taken for upper layer are $N = N_0e^{z/\phi}$, $L = L_0e^{z/\phi}$ and $\rho_0 = \rho_0e^{z/\phi}$ and for the sandwiched layer, the variations are $N = N_1a^z$, $L = L_1a^z$ and $\rho_1 = \rho_1a^z$ whereas variations taken in the lower half-space are $N = N_2(1 + \alpha z)$, $L = L_2(1 + \beta z)$, $P = P_2(1 + \gamma z)$ and $\rho_2 = \rho_2(1 + \delta z)$ where ϕ is a constant having a dimension equal to length and a, α, β, γ and δ are constants having dimensions equal to the inverse of length. Here N_1 and L_1 are the elastic moduli along the direction of r– and z– axis respectively and ρ_1 is the density of the sandwiched layer. N_i and L_i, $i = 0, 2$ are the directional rigidities, ρ_i, $i = 0, 2$ are the densities of the upper layer and the half-space respectively. P is the initial stress at any point in the half-space. The upper layer and half-space are assumed to be transversely isotropic with z–axis as the axis of symmetry.

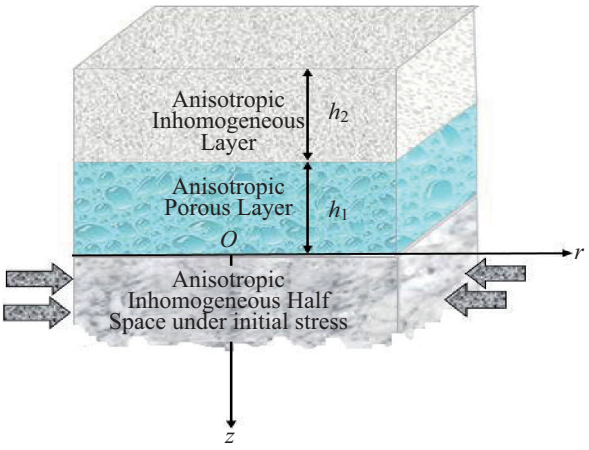


Fig. 1 Geometry of the problem.

2.1 Solution of the Sandwiched Anisotropic Porous Layer

Let r and θ be the radial and circumferential coordinates respectively. Propagation of torsional surface wave in the radial direction and all its mechanical properties are independent of θ. Let (u_1, v_1, w_1) and (U_1, V_1, W_1) be the components of displacement vector of solid and liquid parts of porous layer respectively, and the propagation of torsional surface wave be represented by the displacement components as $u_1 = w_1 = 0 = U_1 = W_1$, $v_1 = v_1(r, z, t)$ and $V_1 = V_1(r, z, t)$.

The equation of motion for the anisotropic porous layer in the absence of body force is given by Biot [22] as

$$\begin{aligned}&\frac{\partial\sigma_{r\theta}}{\partial r}+\frac{\partial\sigma_{z\theta}}{\partial z}+2\frac{\sigma_{r\theta}}{r}=\frac{\partial^2}{\partial t^2}\left(\rho_{rr}v_1+\rho_{r\theta}V_1\right),\\&\frac{\partial^2}{\partial t^2}\left(\rho_{r\theta}v_1+\rho_{\theta\theta}V_1\right)=0.\end{aligned}\tag{1}$$

Here σ_{ij} are the stress components of solid. For an isotropic porous medium, the stress-strain relations are as follows:

$$\begin{aligned}&\sigma_{r\theta}=2Ne_{r\theta},\quad \sigma_{z\theta}=2Le_{z\theta},\\&e_{r\theta}=\frac{1}{2}\left(\frac{\partial v_1}{\partial r}-\frac{v_1}{r}\right),\quad e_{z\theta}=\frac{1}{2}\frac{\partial v_1}{\partial z},\end{aligned}\tag{2}$$

Here, the mass coefficients ρ_{rr}, $\rho_{r\theta}$ and $\rho_{\theta\theta}$ are related to the densities ρ_1, ρ_s and ρ_w, respectively by the relation.

$$\rho_{rr}+\rho_{r\theta}=(1-f)\rho_s,\rho_{r\theta}+\rho_{\theta\theta}=f\rho_w,$$

so that the mass density of the bulk material is

$$\begin{aligned}\rho_1&=\rho_{rr}+2\rho_{r\theta}+\rho_{\theta\theta}\\&=\left(\rho_{rr}+\rho_{r\theta}\right)+\left(\rho_{r\theta}+\rho_{\theta\theta}\right)\\&=\rho_s+f\left(\rho_w-\rho_s\right).\end{aligned}\tag{3}$$

https://doi.org/10.1017/jmech.2017.1 Published online by Cambridge University Press

Biot [9, 10] investigated that the mass coefficients obey the following inequalities:

$$\rho_{rr} > 0, \quad \rho_{r\theta} < 0, \quad \rho_{\theta\theta} > 0, \quad \rho_{rr}\rho_{\theta\theta} - \rho_{r\theta}^2 > 0$$

Using the above relation and from Eq. (1) and Eq. (2), we obtained

$$N\left(\frac{\partial^2 v_1}{\partial r^2} + \frac{1}{r}\frac{\partial v_1}{\partial r} - \frac{v_1}{r^2}\right) + \frac{\partial}{\partial z}\left(L\frac{\partial v_1}{\partial z}\right) = d'\frac{\partial^2 v_1}{\partial t^2}, \tag{4}$$

where $d' = \rho_{rr} - \dfrac{\rho_{r\theta}^2}{\rho_{\theta\theta}}$.

Now, the solution of Eq. (4) can be assumed as

$$v_1 = V_1(z)J_1(kr)e^{i\omega t}, \tag{5}$$

Now, from Eq. (4) and Eq. (5), we get

$$\frac{d^2V_1}{dz^2} + \frac{1}{L}\frac{dL}{dz}\frac{dV_1}{dz} - \frac{k^2N}{L}\left(1 - \frac{d\rho_1 c^2}{N}\right)V_1 = 0, \tag{6}$$

Here $d = \dfrac{d'}{\rho_1}$ and parameters may be non-dimensional as

$$\gamma_{11} = \frac{\rho_{rr}}{\rho_1}, \quad \gamma_{12} = \frac{\rho_{r\theta}}{\rho_1}, \quad \gamma_{22} = \frac{\rho_{\theta\theta}}{\rho_1}, \quad \text{and}$$

$$d = \frac{d'}{\rho_1} = \frac{1}{\rho_1}\left(\rho_{rr} - \frac{\rho_{r\theta}^2}{\rho_{\theta\theta}}\right) = \gamma_{11} - \frac{\gamma_{12}^2}{\gamma_{22}}.$$

Thus, one gets the following:

(i) $d \to 1$, when the layer is a non- porous solid.

(ii) $d \to 0$, when the layer is fluid.

(iii) $0 < d < 1$, when the layer is poroelastic.

Using $V_1 = \dfrac{\delta_1}{\sqrt{L}}$, Eq. (6) can be written as

$$\frac{d^2\delta_1}{dz^2} - \frac{1}{2L}\left[\frac{d^2L}{dz^2} - \frac{1}{2L}\left(\frac{dL}{dz}\right)^2\right]\delta_1 - \frac{k^2N}{L}\left(1 - \frac{d\rho_1 c^2}{N}\right)\delta_1 = 0. \tag{7}$$

Now, the variations in elastic moduli and density in the layer has been taken as

$$N = N_1 a^z, \quad L = L_1 a^z, \quad \rho_1 = \rho_1 a^z \tag{8}$$

Using Eq. (8), Eq. (7) becomes

$$\frac{d^2\delta_1}{dz^2} - \left[\frac{(\log a)^2}{4} + \frac{k^2N_1}{L_1}\left(1 - \frac{d\rho_1 c^2}{N_1}\right)\right]\delta_1 = 0, \tag{9}$$

implies that

$$\frac{d^2\delta_1}{dz^2} + m_1^2\delta_1 = 0, \tag{10}$$

where $m_1^2 = k^2\left[\dfrac{N_1}{L_1}\left(\dfrac{dc^2}{c_1^2} - 1\right) - \dfrac{(\log a)^2}{4k^2}\right]$ and $c_1 = \sqrt{\dfrac{N_1}{\rho_1}}$ = shear wave velocity in the sandwiched layer.

The solution of Eq. (10) is obtained as

$$\delta_1(z) = A_1 e^{-im_1 z} + B_1 e^{im_1 z}, \tag{11}$$

where, A_1 and B_1 are arbitrary constants.

Thus, the displacement in the anisotropic porous layer is

$$v_1 = \frac{\left(A_1 e^{-im_1 z} + B_1 e^{im_1 z}\right)}{\sqrt{L_1}} e^{-\frac{z}{2}\log a} J_1(kr)e^{i\omega t}. \tag{12}$$

2.2 Solution for the Inhomogeneous Anisotropic Upper Medium

The dynamic equation of motion for the inhomogeneous anisotropic medium is given as Biot [22]

$$\frac{\partial \sigma_{r\theta}}{\partial r} + \frac{\partial \sigma_{z\theta}}{\partial z} + 2\frac{\sigma_{r\theta}}{r} = \rho_0\frac{\partial^2 v_0}{\partial t^2}, \tag{13}$$

where, $v_0 = v_0(r, z, t)$ is the displacement along θ direction.

For a non-homogeneous anisotropic elastic medium, the following relations relate stress to strain:

$$\sigma_{r\theta} = 2Ne_{r\theta}, \quad \sigma_{z\theta} = 2Le_{z\theta},$$
$$e_{r\theta} = \frac{1}{2}\left(\frac{\partial v_0}{\partial r} - \frac{v_0}{r}\right), \quad e_{z\theta} = \frac{1}{2}\frac{\partial v_0}{\partial z}, \tag{14}$$

From Eq. (13) and Eq. (14), we get

$$N\left(\frac{\partial^2 v_0}{\partial r^2} + \frac{1}{r}\frac{\partial v_0}{\partial r} - \frac{v_0}{r^2}\right) + \frac{\partial}{\partial z}\left(L\frac{\partial v_0}{\partial z}\right) = \rho_0\frac{\partial^2 v_0}{\partial t^2}. \tag{15}$$

Now, a harmonic wave propagating along r– direction may be considered as of the form

$$v_0 = V_0(z)J_1(kr)e^{i\omega t}, \tag{16}$$

In view of Eq. (16), Eq. (15) reduces to

$$\frac{d^2V_0}{dz^2} + \frac{1}{L}\frac{dL}{dz}\frac{dV_0}{dz} - \frac{k^2N}{L}\left(1 - \frac{\rho_0 c^2}{N}\right)V_0 = 0. \tag{17}$$

On substituting $V_0 = \dfrac{\delta_0}{\sqrt{L}}$, in equation (17), we get

$$\frac{d^2\delta_0}{dz^2} - \frac{1}{2L}\left[\frac{d^2L}{dz^2} - \frac{1}{2L}\left(\frac{dL}{dz}\right)^2\right]\delta_0 - \frac{k^2N}{L}\left(1 - \frac{\rho_0 c^2}{N}\right)\delta_0 = 0. \tag{18}$$

https://doi.org/10.1017/jmech.2017.1 Published online by Cambridge University Press

Now, the variations in directional rigidities and density in the upper layer have been taken as:

$$N = N_0 e^{z/\phi}, \quad L = L_0 e^{z/\phi}, \quad \rho_0 = \rho_0 e^{z/\phi} \tag{19}$$

where ϕ is the inhomogeneity parameter associated to the elastic constants and density of the upper layer.

Using Eq. (19), Eq. (18) takes the form

$$\frac{d^2\delta_0}{dz^2} - m_0^2\delta_0 = 0, \tag{20}$$

where $m_0^2 = k^2\left[\frac{1}{4\phi^2k^2} + \frac{N_0}{L_0}\left(1 - \frac{c^2}{c_0^2}\right)\right]$ and $c_0 = \sqrt{\frac{N_0}{\rho_0}} =$ is the shear wave velocity in the upper layer.

The solution of Eq. (20) is given by

$$\delta_0(z) = A_0 e^{-m_0 z} + B_0 e^{m_0 z}, \tag{21}$$

where A_0 and B_0 are arbitrary constants and hence displacement in the upper inhomogeneous layer is given by

$$v_0 = \frac{\left(A_0 e^{-\left(m_0 + \frac{1}{2\phi}\right)z} + B_0 e^{\left(m_0 - \frac{1}{2\phi}\right)z}\right)}{\sqrt{L_0}} J_1(kr) e^{i\omega t}. \tag{22}$$

2.3 Solution for the Initially Stressed Inhomogeneous Anisotropic Half-Space

The equation of motion for the half-space as given by Biot [23] is

$$N\left(\frac{\partial^2 v_2}{\partial r^2} + \frac{1}{r}\frac{\partial v_2}{\partial r} - \frac{v_2}{r^2}\right) + \frac{\partial}{\partial z}\left(\left(L - \frac{P}{2}\right)\frac{\partial v_2}{\partial z}\right) = \rho_2 \frac{\partial^2 v_2}{\partial t^2}. \tag{23}$$

Now the variation in rigidities, density and initial stress are considered as

$$\begin{aligned} N &= N_2(1+\alpha z), \quad L = L_2(1+\beta z), \\ P &= P_2(1+\gamma z), \quad \rho = \rho_2(1+\delta z). \end{aligned} \tag{24}$$

The solution of Eq. (23) may be taken as

$$v_2 = V_2(z) J_1(kr) e^{i\omega t}, \tag{25}$$

With the help of Eqs. (24) and (25), Eq. (23) gets the form as

$$\frac{d^2V_2}{dz^2} + \frac{\left[L_2\beta - \frac{P_2\gamma}{2}\right]}{\left[L_2(1+\beta z) - \frac{P_2(1+\gamma z)}{2}\right]}\frac{dV_2}{dz} - \frac{N_2k^2}{\left[L_2(1+\beta z) - \frac{P_2(1+\gamma z)}{2}\right]}\left\{(1+\alpha z) - \frac{c^2}{c_2^2}(1+\delta z)\right\}V_2(z) = 0, \tag{26}$$

where $c_2 = \sqrt{\frac{N_2}{\rho_2}} =$ is the shear wave velocity in the upper layer.

Now substituting $V_2(z) = \frac{\psi(z)}{\sqrt{\left(L_2 - \frac{P_2}{2}\right) + \left(L_2\beta - \frac{P_2\gamma}{2}\right)z}}$ in Eq. (26), we have

$$\psi''(z) + \frac{1}{4}\frac{\left(L_2\beta - \frac{P_2\gamma}{2}\right)^2}{\left[\left(L_2 - \frac{P_2}{2}\right) + \left(L_2\beta - \frac{P_2\gamma}{2}\right)z\right]^2}\psi(z) - \frac{N_2k^2}{\left[\left(L_2 - \frac{P_2}{2}\right) + \left(L_2\beta - \frac{P_2\gamma}{2}\right)z\right]}\left\{\left(1 - \frac{c^2}{c_2^2}\right) + \left(\alpha - \frac{c^2}{c_2^2}\delta\right)z\right\}\psi(z) = 0. \tag{27}$$

Again substituting $\psi(z) = \psi_1(\eta)$ and $\eta = \frac{2k\gamma_1\left[\left(L_2 - \frac{P_2}{2}\right) + \left(L_2\beta - \frac{P_2\gamma}{2}\right)z\right]}{\left(L_2\beta - \frac{P_2\gamma}{2}\right)}$, then Eq. (27) becomes

$$\psi_1''(\eta) + \left[\frac{1}{4\eta^2} + \frac{R}{\eta} - \frac{1}{4}\right]\psi_1(\eta) = 0, \tag{28}$$

where R and γ_1^2 are given in Appendix A.

Eq. (28) is known as the Whittaker equation and the solution is given by

$$\psi_1(\eta) = D_1 W_{R,0}(\eta) + D_2 W_{-R,0}(-\eta) \tag{29}$$

where D_1 and D_2 are arbitrary constants and $W_{R,0}(\eta)$ is the Whittaker function.

The solution of Eq. (29) satisfying the condition that $\lim_{z\to\infty} V_2(z) \to 0$ i.e. $\lim_{\eta\to\infty} \psi(\eta) \to 0$ may be taken as

https://doi.org/10.1017/jmech.2017.1 Published online by Cambridge University Press

$$\psi_1(\eta) = D_1 W_{R,0}(\eta). \tag{30}$$

Expanding the Whittaker function up to a linear term, we obtain the displacement of the torsional surface wave for the lower half- space

$$v_2 = \frac{D_1 J_1(kr) e^{i\omega t}}{\sqrt{\left(L_2 - \frac{P_2}{2}\right) + \left(L_2\beta - \frac{P_2\gamma}{2}\right) z}} e^{-\frac{\eta}{2}} [\eta]^{1/2} \left[1 + \frac{\eta}{2} - R\eta\right]. \tag{31}$$

3. BOUNDARY CONDITIONS AND DISPERSION RELATION

The suitable boundary conditions, according to the formulation of the problem are as follows:

(i) At the interface $z = -(h_1 + h_2)$, stress component is

$$L_0 \frac{\partial v_0}{\partial z} = 0. \tag{32}$$

(ii) Displacements and stresses are continuous at the interface $z = -h_1$.

$$v_0 = v_1. \tag{33}$$

$$L_0 e^{\frac{-h_1}{\phi}} \frac{\partial v_0}{\partial z} = L_1 a^{-h_1} \frac{\partial v_1}{\partial z}. \tag{34}$$

(iii) At the interface $z = 0$, displacements and stresses are continuous

$$v_1 = v_2. \tag{35}$$

$$L_1 \frac{\partial v_1}{\partial z} = L_2 \frac{\partial v_2}{\partial z}. \tag{36}$$

Using Eq. (22) and boundary condition (32), we get

$$\sqrt{L_0}\left\{-A_0\left(m_0 + \frac{1}{2\phi}\right)e^{\left(m_0+\frac{1}{2\phi}\right)(h_1+h_2)} + B_0\left(m_0 - \frac{1}{2\phi}\right)e^{-\left(m_0-\frac{1}{2\phi}\right)(h_1+h_2)}\right\} = 0. \tag{37}$$

In view of Equations (22) and (12), boundary conditions (33) and (34) result in

$$A_0 \frac{e^{\left(m_0+\frac{1}{2\phi}\right)h_1}}{\sqrt{L_0}} + B_0 \frac{e^{-\left(m_0-\frac{1}{2\phi}\right)h_1}}{\sqrt{L_0}} - e^{\frac{h_1}{2}\log a}\left[\frac{e^{im_1h_1}}{\sqrt{L_1}}A_1 + \frac{e^{-im_1h_1}}{\sqrt{L_1}}B_1\right] = 0. \tag{38}$$

$$\begin{aligned}&\sqrt{L_0}\left[-\left(m_0 + \frac{1}{2\phi}\right)e^{\left(m_0-\frac{1}{2\phi}\right)h_1}A_0 + \left(m_0 - \frac{1}{2\phi}\right)e^{-\left(m_0+\frac{1}{2\phi}\right)h_1}B_0\right]\\ &-\sqrt{L_1}\left[-\left(im_1 + \frac{\log a}{2}\right)e^{\left(im_1-\frac{\log a}{2}\right)h_1}A_1 + \left(im_1 - \frac{\log a}{2}\right)B_1 e^{-\left(im_1+\frac{\log a}{2}\right)h_1}\right] = 0.\end{aligned} \tag{39}$$

Using boundary conditions (35) and (36) in Equations (12) and (31), we get

$$\left[\frac{1}{\sqrt{L_1}}A_1 + \frac{1}{\sqrt{L_1}}B_1\right] - M_1 D_1 = 0. \tag{40}$$

$$\sqrt{L_1}\left[-\left(im_1 + \frac{\log a}{2}\right)A_1 + \left(im_1 - \frac{\log a}{2}\right)B_1\right] - kL_2M_2D_1 = 0, \tag{41}$$

where M_1 and M_2 are given in Appendix B.

Now, eliminating A_0, B_0, A_1, B_1 and D_1 from Equations (37) to (41), we have

$$\begin{vmatrix} -\psi_3 \times e^{\psi_3(h_1+h_2)} & \psi_2 \times e^{-\psi_2(h_1+h_2)} & 0 & 0 & 0 \\ \frac{e^{\psi_3 h_1}}{\sqrt{L_0}} & \frac{e^{-\psi_2 h_1}}{\sqrt{L_0}} & -e^{\frac{h_1}{2}\log a}\frac{e^{im_1h_1}}{\sqrt{L_1}} & -e^{\frac{h_1}{2}\log a}\frac{e^{-im_1h_1}}{\sqrt{L_1}} & 0 \\ -\sqrt{L_0}\psi_3 e^{\psi_2 h_1} & \sqrt{L_0}\psi_2 e^{-\psi_3 h_1} & \sqrt{L_1}e^{-\frac{h_1}{2}\log a}T_1 e^{im_1h_1} & -\sqrt{L_1}e^{-\frac{h_1}{2}\log a}T_2 e^{-im_1h_1} & 0 \\ 0 & 0 & \frac{1}{\sqrt{L_1}} & \frac{1}{\sqrt{L_1}} & -M_1 \\ 0 & 0 & -\sqrt{L_1}T_1 & \sqrt{L_1}T_2 & -kL_2M_2 \end{vmatrix} = 0,$$

where ψ_2, ψ_3, T_1 and T_2 are given in Appendix C.

Expanding the above determinant, we obtain

https://doi.org/10.1017/jmech.2017.1 Published online by Cambridge University Press

$$\tan kh_1\sqrt{\frac{N_1}{L_1}\left(\frac{dc^2}{c_1^2}-1\right)-\frac{(\log a)^2}{4k^2}}=\frac{S_1}{S_2}, \tag{42}$$

where S_1 and S_2 are defined in Appendix C.

Eq. (42) gives the required dispersion equation of torsional surface wave in an anisotropic porous layer lying between the anisotropic inhomogeneous layer and an initially stressed anisotropic inhomogeneous half- space.

4. PARTICULAR CASES

4.1 Case 1

When the directional rigidities and densities in the upper layer become constants i.e. $\frac{1}{\phi}\to 0$ and $N_0 = L_0$, then Eq. (42) reduces to

$$\tan kh_1\sqrt{\frac{N_1}{L_1}\left(\frac{dc^2}{c_1^2}-1\right)-\frac{(\log a)^2}{4k^2}}$$
$$=\frac{4e^{h_1\log a}k^2\tanh kh_2\sqrt{\left(1-\frac{c^2}{c_0^2}\right)}\left(1-\frac{c^2}{c_0^2}\right)-\frac{2kL_2}{L_0}\frac{M_2}{M_1}2m_1k\sqrt{\left(1-\frac{c^2}{c_0^2}\right)}}{e^{h_1\log a}4k^2\tanh kh_2\sqrt{\left(1-\frac{c^2}{c_0^2}\right)}\left(1-\frac{c^2}{c_0^2}\right)\left\{\frac{\log a}{2}+\frac{kL_2}{L_1}\frac{M_2}{M_1}\right\}+k\sqrt{\left(1-\frac{c^2}{c_0^2}\right)}\left\{\frac{L_1}{L_0}\left(\log a^2+4m_1^2\right)+\frac{4kL_2}{L_0}\frac{M_2}{M_1}\frac{\log a}{2}\right\}}, \tag{43}$$

Eq. (43) is the dispersion equation of torsional surface wave in an anisotropic porous layer lying between homogeneous isotropic upper layer and an initially stressed anisotropic inhomogeneous half-space.

4.2 Case 2

When the sandwiched layer is a homogeneous, isotropic and nonporous solid, i.e. $\log a \to 0$, $d \to 1$ and $N_1 = L_1$, then eq. (42) takes the form

$$\tan kh_1\sqrt{\left(\frac{c^2}{c_1^2}-1\right)}=\frac{4\tanh m_0h_2\left(m_0^2-\frac{1}{4\phi^2}\right)k\sqrt{\left(1-\frac{c^2}{c_1^2}\right)}-\frac{2kL_2}{L_0}\frac{M_2}{M_1}e^{\frac{h_1}{\phi}}\left(2m_0+\frac{\tanh m_0h_2}{\phi}\right)k\sqrt{\left(\frac{c^2}{c_1^2}-1\right)}}{\left\{\frac{2kL_2}{L_1}\frac{M_2}{M_1}\frac{\tanh m_0h_2}{2}\left\{4m_0^2-\frac{1}{\phi^2}\right\}\right\}+e^{\frac{h_1}{\phi}}\left\{\frac{L_1}{L_0}\left(m_0+\frac{1}{2\phi}\tanh m_0h_2\right)4k^2\left(\frac{c^2}{c_1^2}-1\right)\right\}}, \tag{44}$$

which is the dispersion equation of the torsional surface wave in a nonporous, homogeneous isotropic layer lying between two anisotropic inhomogeneous medium.

4.3 Case 3

When all the inhomogeneity in the half-space tend to zero i.e. $\alpha \to 0$, $\beta \to 0$, $\gamma \to 0$, $\delta \to 0$, $P_2 \to 0$ and $N_2 = L_2$ i.e. when the lower half-space becomes isotropic homogeneous and initial stress free, then dispersion equation (42) takes the form

$$\tan kh_1\sqrt{\frac{N_1}{L_1}\left(\frac{dc^2}{c_1^2}-1\right)-\frac{(\log a)^2}{4k^2}}$$
$$=\frac{4e^{h_1\log a}\tanh m_0h_2\left(m_1m_0^2-\frac{m_1}{4\phi^2}\right)+\frac{2kL_2}{L_0}\sqrt{\left(\frac{c^2}{c_2^2}-1\right)}e^{\frac{h_1}{\phi}}\left(2m_1m_0+\frac{m_1\tanh m_0h_2}{\phi}\right)}{\begin{aligned}&e^{h_1\log a}\left\{4m_0^2\tanh m_0h_2\frac{\log a}{2}-\tanh m_0h_2\frac{\log a}{2}\frac{1}{\phi^2}-\frac{2kL_2}{L_1}\sqrt{\left(\frac{c^2}{c_2^2}-1\right)}\frac{\tanh m_0h_2}{2}\left\{4m_0^2-\frac{1}{\phi^2}\right\}\right\}\\&+e^{\frac{h_1}{\phi}}\left\{\frac{L_1}{L_0}\left(m_0+\frac{1}{2\phi}\tanh m_0h_2\right)\left(\log a^2+4m_1^2\right)-\frac{2kL_2}{L_0}\sqrt{\left(\frac{c^2}{c_2^2}-1\right)}\frac{\log a}{2}\left(2m_0+\frac{\tanh m_0h_2}{\phi}\right)\right\}\end{aligned}}, \tag{45}$$

https://doi.org/10.1017/jmech.2017.1 Published online by Cambridge University Press

Table 1. Values for dimensionless parameter

Dimensionless parameter	Fig. 2(a)	Fig. 2(b)	Fig. 3(a)	Fig. 3(b)	Fig. 4(a)	Fig. 4(b)	Fig. 5(a)	Fig. 5(b)	Fig. 6
ϕk	–	0.2	0.2	0.2	0.2	0.2	0.2	0.2	0.2
log $a/2k$	0.3	–	0.3	0.3	0.3	0.3	0.3	0.3	0.3
α/k	0.2	0.2	–	0.2	0.2	0.2	0.2	0.2	0.2
β/k	0.5	0.5	0.5	–	0.5	0.5	0.5	0.5	0.5
δ/k	0.3	0.3	0.3	0.3	–	0.3	0.3	0.3	0.3
γ/k	0.2	0.2	0.2	0.2	0.2	–	0.2	0.2	0.2
d	0.6	0.6	0.6	0.6	0.6	0.6	0.6	0.6	–
ξ	0.4	0.4	0.4	0.4	0.4	0.4	–	–	0.4
kh_2	0.2	0.2	0.2	0.2	0.2	0.2	0.2	0.2	0.2

which is the dispersion equation of the torsional surface wave in an anisotropic porous layer lying between anisotropic inhomogeneous medium and isotropic homogeneous half-space.

4.4 Case 4

When neglecting the upper medium, i.e. $h_2 \to 0$, and sandwiched layer and lower half-space are isotropic and homogeneous, and $N_2 = L_2 = \mu_2$ and $N_1 = L_1 = \mu_1$ then equation (42) takes the form

$$\tan kh_1\sqrt{\left(\frac{c^2}{c_1^2}-1\right)} = \frac{\mu_2\sqrt{\left(1-\frac{c^2}{c_2^2}\right)}}{\mu_1\sqrt{\left(\frac{c^2}{c_1^2}-1\right)}}. \tag{46}$$

which is the well-known classical Love wave Equation.

5. NUMERICAL CALCULATION AND RESULTS

To demonstrate the effects of dimensionless inhomogeneity parameter associated with all the three medium, poroelastic constant, dimensionless initial stress, on the propagation of the torsional surface wave, some numerical computation have been done and illustrated them graphically. The different values of the parameters have been considered to represent the characteristics of the dispersion equation (42). For the graphical representation, numerical values of various parameters and elastic constants have been taken from Chattopadhyay *et al.* [24], Samal and Chattaraj [25] and Tierstein [26], and which are as follows:

For upper layer

$$N_0 = 6\times10^9\, N/m^2, \quad L_0 = 7.5\times10^9\, N/m^2,$$
$$\rho_0 = 3364\ kg/m^3,$$

For sandwiched layer

$$N_1 = 0.2765\times10^{10}\, N/m^2, \quad L_1 = 0.1387\times10^{10}\, N/m^2,$$
$$\rho_{11}=1.926137\times10^3\ kg/m^2, \quad \rho_{12}=-0.002137\times10^3\ kg/m^2,$$
$$\rho_{22}=0.215337\times10^3\ kg/m^2, \quad \rho_1 = 7800\ kg/m^3,$$

For lower half-space

$$N_2 = 39.9\times10^9\, N/m^2, \quad L_2 = 57.9\times10^9\, N/m^2,$$
$$\rho_2 = 2649\ kg/m^3.$$

The values of inhomogeneity parameters, initial stress and poroelastic constants for all the figures have been taken from Table 1 and results have been generated. The results have been examined through Figs. 2 to Fig. 6. All these figures show the variation of dimensionless phase velocity against dimensionless wave number.

Figure 2(a) renders the dispersion curve for the torsional surface wave by taking the values of the dimensionless inhomogeneity parameter associated with the upper layer, i.e. ϕk as 0.1, 0.3, 0.5, 0.7 and 0.9 for the curve numbers 1, 2, 3, 4, and 5 respectively. The following observations have been proliferated:

(i) Here, it can be seen that the phase velocity decreases with increasing value of the inhomogeneity parameter associated with the upper layer.

(ii) The phase velocity is more prominent at the low frequency region and becomes closer to each other with increasing magnitude of wave number i.e. at high frequencies.

Figure 2(b) portrays the effect of dimensionless inhomogeneity parameter associated with the sandwiched layer i.e. (log $a/2k$). In this case, the value of log $a/2k$ is taken as 0.1, 0.2, 0.3, 0.4 and 0.5 for the curve numbers 1, 2, 3, 4, 5 and 6 respectively. The curves have been plotted in the similar manner as before. The following points have been noted:

(i) The phase velocity increases with the increasing magnitude of inhomogeneity parameter at a particular frequency.

(ii) The curves are equally apart from each other and the slope of the curves are uniformly distributed.

https://doi.org/10.1017/jmech.2017.1 Published online by Cambridge University Press

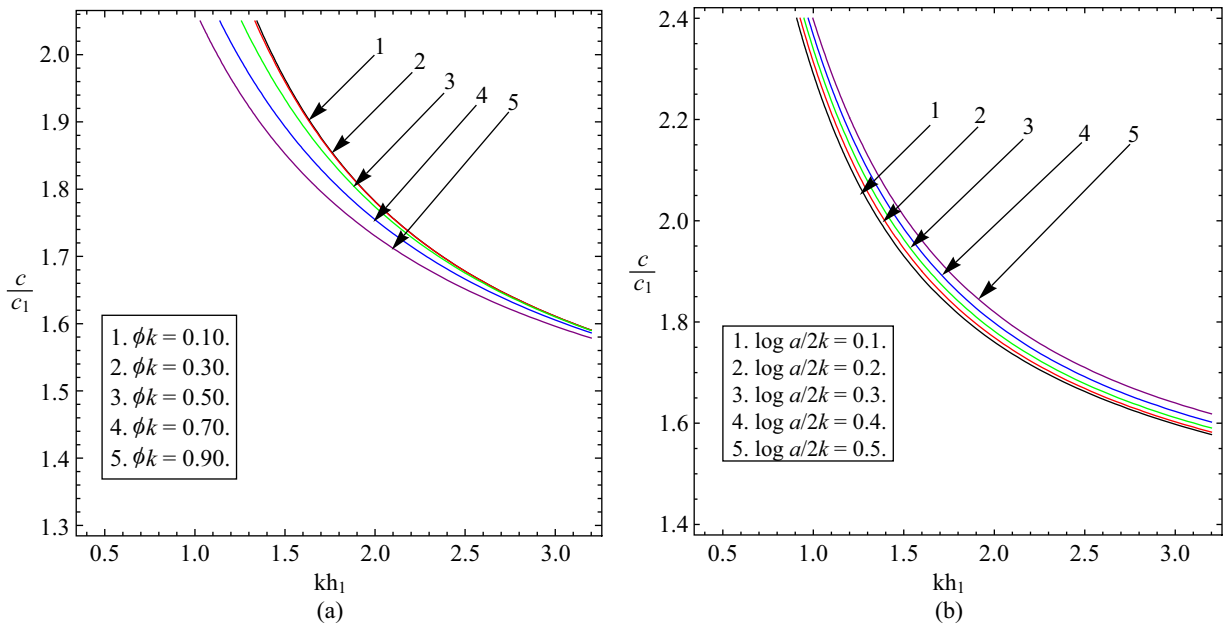


Fig. 2 Variation of dimensionless phase velocity against non-dimensional wave number (a) for different values of inhomogeneity parameter (φk) and (b) for different values of inhomogeneity parameter (log $a/2k$).

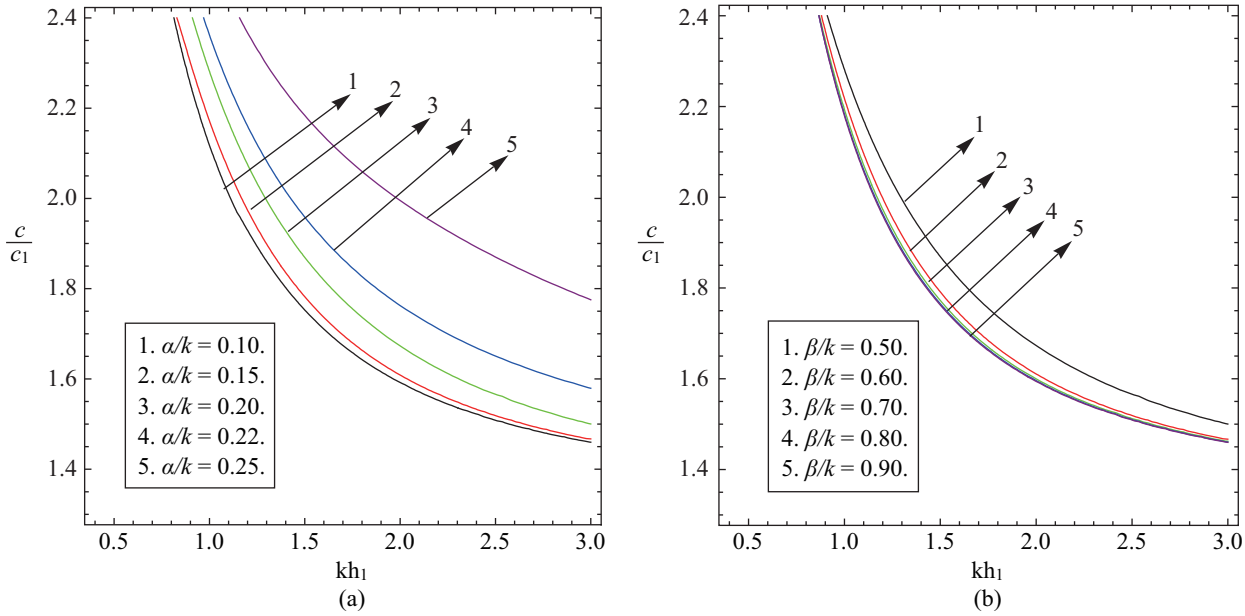


Fig. 3 Variation of dimensionless phase velocity against a non-dimensional wave number (a) for different values of inhomogeneity parameter (α/k) and (b) for different values of inhomogeneity parameter (β/k).

Figure 3(a) has been plotted to depict the effect of dimensionless inhomogeneity parameter related to half-space i.e. (α/k) on the dispersion curves for the torsional surface wave. The increasing value of α/k has been taken into account in the anisotropic inhomogeneous half-space. The values for α/k are taken as 0.10, 0.15, 0.20, 022 and 0.25 for the curve numbers. 1, 2, 3, 4 and 5 respectively. The following observations have been found:

(i) It is concluded from the figure, that increasing magnitude of inhomogeneity parameter put a significant impact on the phase velocity. The phase velocity is increased when inhomogeneity parameter, α/k is increased.

(ii) In the low frequency region, the curves are little bit closer to the each other and get scattered in the higher frequency region revealing the fact that this inhomogeneity parameter enlarge the phase velocity.

Figure 3(b) studies the consequence of inhomogeneity parameter corresponding to the lower anisotropic inhomogeneous half-space i.e. (β/k). The values of β/k for

https://doi.org/10.1017/jmech.2017.1 Published online by Cambridge University Press

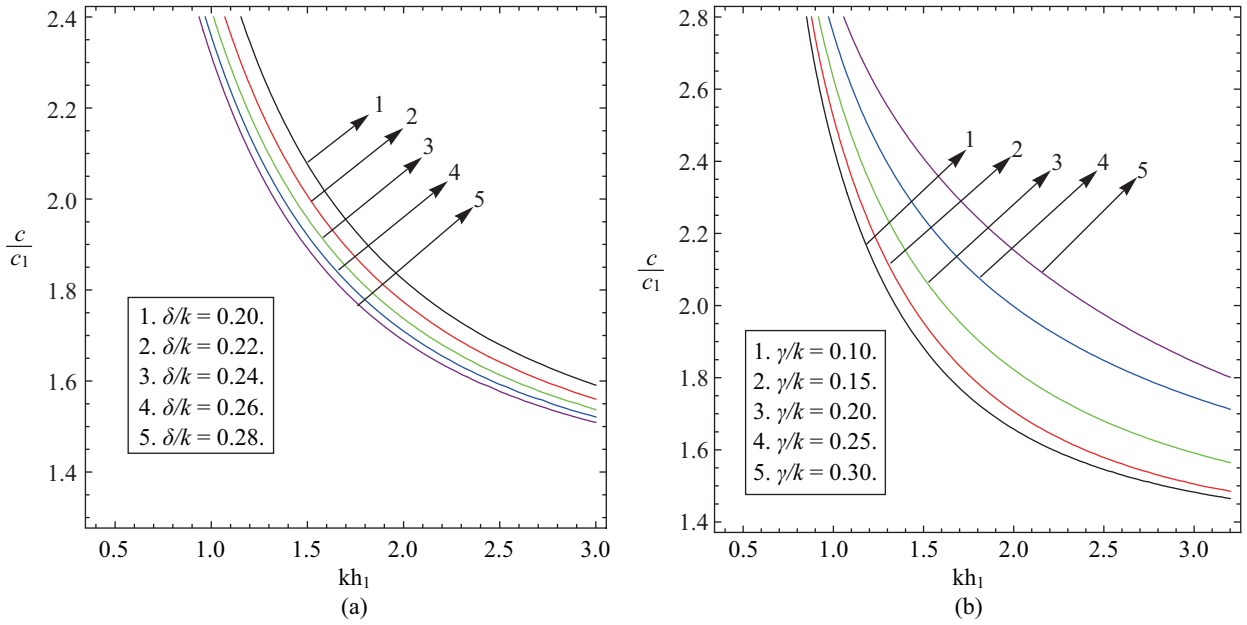


Fig. 4 Variation of dimensionless phase velocity against a non-dimensional wave number (a) for different values of inhomogeneity parameter (δ/k) and (b) for different values of inhomogeneity parameter (γ/k).

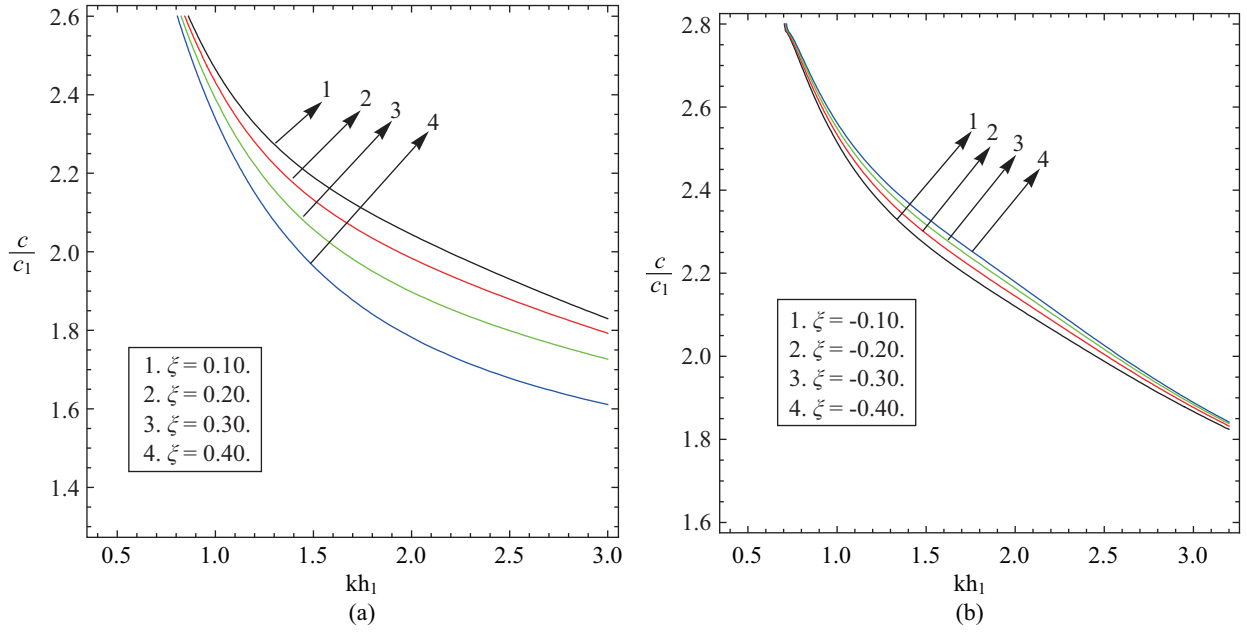


Fig. 5 Variation of dimensionless phase velocity against a non-dimensional wave number (a) for different value of compressive initial stress ($\xi > 0$) and (b) for different values of tensile initial stress ($\xi < 0$).

the curve numbers 1, 2, 3, 4 and 5 have been taken as 0.50, 0.60, 0.70, 0.80 and 0.90 respectively.

The following facts are enlightened:

(i) The phase velocity get decreased with the increasing extent of inhomogeneity parameter at a particular frequency.

(ii) The curves are likely to coincide with each other for higher magnitude of inhomogeneity parameter.

In Fig. 4(a), an attempt has been made to show the effect of inhomogeneity parameter (δ/k) associated with density in the lower anisotropic half-space. The values of δ/k for the curve numbers 1, 2, 3, 4 and 5 have been taken as 0.20, 0.22, 0.24, 0.26 and 0.28 respectively.

(i) From this figure, it is noticed that the phase velocity decreases with increasing magnitude of inhomogeneity parameter.

(ii) The curves remain apart from each other to the same extent at any particular frequency and the uniform slopes of all the curves put a prominent effect on the phase velocity.

Figure 4(b) studies the effect of inhomogeneity parameter (γ/k) associated with initial stress present in

https://doi.org/10.1017/jmech.2017.1 Published online by Cambridge University Press

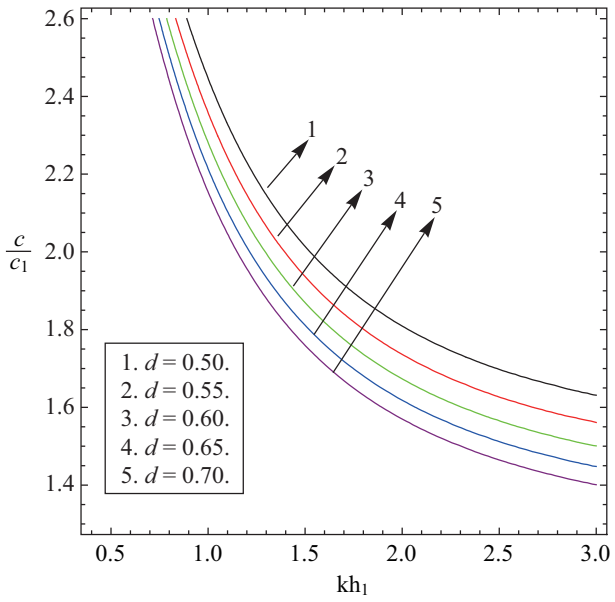


Fig. 6 Variation of dimensionless phase velocity against a non-dimensional wave number for different values of poroelastic constant d.

lower anisotropic inhomogeneous half-space. The values of γ/k for the curve numbers 1, 2, 3, 4 and 5 have been taken as 0.10, 0.15, 0.20, 0.25 and 0.30 respectively.

(i) The phase velocity increases with increasing magnitude of inhomogeneity parameter to a greater extent of frequency.

(ii) The differences between the curves, gradually increase with the increasing frequency and the phase velocity of torsional surface wave has a prominent effect to be observed at higher frequency.

Figure 5(a) helps to study the dispersion curve when compressive initial stress $\left(\xi = \frac{P_2}{2L_2} > 0\right)$ has been taken into account in the anisotropic inhomogeneous half-space. Here the magnitude of compressive initial stress have been taken as 0.1, 0.2, 0.3 and 0.4 for the curves 1, 2, 3 and 4 respectively.

(i) From this figure, it has been seen that the compressive initial stress has a prominent effect on phase velocity. The phase velocity has been decreased as the magnitude of compressive initial stress is increased.

(ii) Initially, the curves seem to coincide with each other at low frequency, while a great variation is to be observed at higher frequencies.

Figure 5(b) illustrates the impact of tensile initial stress $\left(\xi = \frac{P_2}{2L_2} < 0\right)$ associated with the lower anisotropic inhomogeneous half-space on the dispersion curve. The magnitude of tensile initial stress of have been considered as –0.1, –0.2, –0.3 and –0.4 for the curve numbers 1, 2, 3 and 4 respectively.

(i) The phase velocity get increased for the increasing magnitude of tensile initial stress.

(ii) At low frequency, the curves seem to be coinciding with each other, but at later half, little bit of variation is to be observed but again the curves are likely to meet each other at higher frequencies.

Figure 6 has showed the influence of poroelastic constant d on the phase velocity. The values have been considered as 0.550, 0.55, 0.60, 0.65 and 0.70 for the curve numbers 1, 2, 3, 4 and 5 respectively.

(i) The poroelastic constant has a substantial effect on phase velocity. From this figure, it comes into light that the phase velocity decreases with increasing values of poroelastic constant d. The effects of phase velocity become more considerable with the increasing frequency.

6. CONCLUSIONS

In this paper, an analytical approach is used to investigate the propagation of torsional surface wave in an anisotropic inhomogeneous porous layer of finite thickness sandwiched between the anisotropic inhomogeneous layer and initially stressed anisotropic inhomogeneous half-space. It has been observed that present geometry allows torsional waves to propagate. The compact form of dispersion relation has been obtained which coincides with the classical Love Wave Equation. Dispersion velocity has also been computed numerically, and the effects of inhomogeneity parameters associated with the directional rigidities and density present in all the three medium have been studied. Significant effects of inhomogeneity parameters, poroelastic constant, and initial stress on torsional wave propagation have been observed. Therefore, finally throwing light on some important facts:

(i) The inhomogeneity parameter (ϕk) of the upper layer has a pronounced influence on the propagation of torsional surface waves. It has also been found that the phase velocity decreases when the inhomogeneity parameter (ϕk) associated to the rigidity and density of the upper anisotropic inhomogeneous layer is increased.

(ii) Phase velocity increases with increase in inhomogeneity parameter (log $a/2k$) of the anisotropic porous layer.

(iii) The inhomogeneity parameters associated with the directional rigidities and density, i.e. α/k, β/k, δ/k and γ/k of the lower anisotropic inhomogeneous half-space put a remarkable impact on the dispersion velocity. The parameters (α/k) and (γ/k) favorably affect the dispersive velocity whereas the parameters (β/k) and (δ/k) give a reverse effect on the dispersive velocity.

(iv) The compressive initial stress put an adverse effect whereas the tensile initial stress put a favourable effect on the dispersive velocity.

(v) It has also been found that poroelastic constant (d)

https://doi.org/10.1017/jmech.2017.1 Published online by Cambridge University Press

gives a reverse effect on the phase velocity.

As the actual earth is an inhomogeneous-layered structure and can be considered as a composition of different inhomogeneous layers of different geological parameters and settings, therefore it is more pragmatic to consider the inhomogeneity in the present problem to study the propagation of torsional surface waves in anisotropic inhomogeneous medium. The above investigations thus manifest to have an effective influence on the subjects of seismology as well as earthquake sciences, which aid in modeling of wave propagation. In addition, it would be an injustice if the subject of geophysics is not associated with the above investigation. The present paper can assist in the study of oil and gas exploration in the layered structure of the earth. Disaster prevention and civil engineering can also find some noteworthy applications from this study. Thus, the significance of this present paper is not limited to only one field. Rather, it has a diversified application in the modern world.

ACKNOWLEDGEMENTS

The authors wish to extend a heartfelt acknowledgement to Indian Institute of Technology (ISM), Dhanbad, Jharkhand-826004, India, for rendering all financial assistance and opportunity to Ms. Neelima Bhengra (ISM-JRF).

APPENDIX

Appendix A

$$R=\frac{N_2 k}{2\gamma_1}\left\{\frac{\left(\alpha-\frac{c^2}{c_2^2}\delta\right)\left(L_2-\frac{P_2}{2}\right)-\left(1-\frac{c^2}{c_2^2}\right)\left(L_2\beta-\frac{P_2\gamma}{2}\right)}{\left(L_2\beta-\frac{P_2\gamma}{2}\right)^2}\right\},\quad \gamma_1^2=\frac{N_2\left(\alpha-\frac{c^2}{c_2^2}\delta\right)}{\left(L_2\beta-\frac{P_2\gamma}{2}\right)}. \tag{A1}$$

Appendix B

$$M_1=e^{\frac{-N}{2}}\left\{\frac{2k\gamma_1}{\left(L_2\beta-\frac{P_2\gamma}{2}\right)}\right\}^{1/2}\left[1+\frac{N}{2}-RN\right], \tag{B1}$$

$$M_2=e^{\frac{-N}{2}}\left\{\frac{2k\gamma_1}{\left(L_2\beta-\frac{P_2\gamma}{2}\right)}\right\}^{1/2}\left[R\gamma_1 N-\frac{\gamma_1 N}{2}-2R\gamma_1\right],\quad N=[\eta]_{z=0}=\frac{2k\gamma_1\left(L_2-\frac{P_2}{2}\right)}{\left(L_2\beta-\frac{P_2\gamma}{2}\right)}. \tag{B2}$$

Appendix C

$$\psi_2=\left(m_0-\frac{1}{2\phi}\right),\quad \psi_3=\left(m_0+\frac{1}{2\phi}\right),\quad T_1=\left(im_1+\frac{\log a}{2}\right),\quad T_2=\left(im_1-\frac{\log a}{2}\right). \tag{C1}$$

$$S_1=\left[4e^{h_1\log a}\tanh m_0h_2\left(m_1m_0^2-\frac{m_1}{4\phi^2}\right)-\frac{2kL_2}{L_0}\frac{M_2}{M_1}e^{\frac{h_1}{\phi}}\left(2m_1m_0+\frac{m_1\tanh m_0h_2}{\phi}\right)\right]$$

$$S_2=e^{h_1\log a}\left\{4m_0^2\tanh m_0h_2\frac{\log a}{2}-\tanh m_0h_2\frac{\log a}{2}\frac{1}{\phi^2}+\frac{2kL_2}{L_1}\frac{M_2}{M_1}\frac{\tanh m_0h_2}{2}\left\{4m_0^2-\frac{1}{\phi^2}\right\}\right\}$$

$$+e^{\frac{h_1}{\phi}}\left\{\frac{L_1}{L_0}\left(m_0+\frac{1}{2\phi}\tanh m_0h_2\right)\left(\log a^2+4m_1^2\right)+\frac{2kL_2}{L_0}\frac{M_2}{M_1}\frac{\log a}{2}\left(2m_0+\frac{\tanh m_0h_2}{\phi}\right)\right\} \tag{C2}$$

$$\frac{M_2}{M_1}=\frac{\left[R\gamma_1N-\frac{\gamma_1N}{2}-2R\gamma_1\right]}{\left[1+\frac{N}{2}-RN\right]}.$$

https://doi.org/10.1017/jmech.2017.1 Published online by Cambridge University Press

NOMENCLATURE

$\omega = ck$ = Angular frequency;

c = Phase velocity;

k = Wave number;

$J_1(kr)$ = Bessel's function of the first kind with order one;

ρ_{rr}, $\rho_{r\theta}$ and $\rho_{\theta\theta}$ = mass coefficients;

ρ_1 = density of the anisotropic porous layer;

ρ_0 = density of the upper anisotropic inhomogeneous medium;

ρ_2 = density of the lower anisotropic inhomogeneous half -space;

ρ_s = density of the solid;

ρ_w = density of the water;

f = porosity of the layer;

N, L = shear moduli of the elasticity;

REFERENCES

1. Ewing, W. M., Jardetzky, W. S. and Press, F., *Elastic waves in layered media*, McGraw-Hill, New York (1957).
2. Gubbins, D., *Seismology and Plate Tectonics*, Cambridge University Press, Cambridge (1990).
3. Udias, A., *Principles of Seismology*, Cambridge University Press, Cambridge (1999).
4. Dey, S. and Sarkar, M. G., "Torsional surface waves in an initially stressed anisotropic porous medium," *Journal of Engineering Mechanics*, **128**, pp. 184-189 (2002).
5. Selim, M. M., "Propagation of torsional surface wave in heterogeneous half-space with irregular free surface," *Applied Mathematical Sciences*, **1**, pp. 1429-1437 (2007).
6. Ozturk, A. and Akbarov, S. D., "Torsional wave propagation in a pre-stressed circular cylinder embedded in a pre-stressed elastic medium," *Applied Mathematical Modeling*, **33**, pp. 3636-3649 (2009).
7. Akbarov, S. D., Kepceler, T. and Egilmez, M. M, "Torsional wave dispersion in a finitely pre-strained hollow sandwich circular cylinder," *Journal of Sound and Vibration,* **330**, pp. 4519-4537 (2011).
8. Chattopadhyay, A., Gupta, S., Kumari, P. and Sharma, V. K., "Propagation of torsional waves in an inhomogeneous layer over an inhomogeneous half space," *Meccanica*, **46**, pp. 671-680 (2011).
9. Biot, M. A., "Theory of elastic waves in a fluid-saturated porous solid: I. Low frequency range," *The Journal of the Acoustical Society of America*, **28**, pp. 168-178 (1956).
10. Biot, M. A., "Theory of elastic waves in a fluid-saturated porous solid: II. High frequency range," *The Journal of the Acoustical Society of America*, **28**, pp. 179-191 (1956).
11. Biot, M. A., "Mechanics of deformation and acoustic propagation in porous media," *Journal of Applied Physics,* **33**, pp. 1482-1498 (1962).
12. Deresiewicz, H., "The effect of boundaries on wave propagation in a liquid-filled porous solid: II. The Love waves in a porous layer," *Bulletin of the Seismological Society of America*, **51**, pp. 51-59 (1961).
13. Deresiewicz, H., "The effect of boundaries on wave propagation in a liquid-filled porous solid: VI. The Love waves in a double surface layer," *Bulletin of the Seismological Society of America,* **54**, pp. 417-423 (1964).
14. Deresiewicz, H., "The effect of boundaries on wave propagation in a liquid-filled porous solid: IX. Love waves in a porous internal stratum," *Bulletin of the Seismological Society of America,* **55**, pp. 919-923 (1965).
15. Sharma, M. D. and Gogna, M. L., "Propagation of the Love waves in an initially stressed medium consist of a slow elastic lying over a liquid saturated porous solid half-space," *The Journal of the Acoustical Society of America*, **89** , pp. 2584-2588 (1991).
16. Wang, Y. S. and Zhang Z. M., "Propagation of the Love waves in a transversely isotropic fluid-saturated porous layered half-space," *The Journal of the Acoustical Society of America*, **103**, pp. 695-701 (1998).
17. Gupta, A. K. and Gupta, S., "Torsional surface waves in gravitating anisotropic porous half space," *Mathematics and Mechanics of Solids,* **16**, pp. 445-450 (2011).
18. Ke, L. L., Wang, Y. S. and Zhang, Z. M., "Love waves in an inhomogeneous fluid saturated porous layered half-space with linearly varying properties," *Soil Dynamics and Earthquake Engineering,* **26**, pp. 574-581 (2006).
19. Bullen, K. E., "The problem of the Earth's density variation," *Bulletin of the Seismological Society of America,* **30**, pp. 235-250 (1940).
20. Gupta, S., Majhi, D. K. and Vishwakarma, S. K., "Torsional surface wave propagation in an initially stressed non-homogeneous layer over a non-homogeneous half-space." *Applied Mathematics and Computation,* **219**, pp. 3209-3218 (2012).
21. Sari, C. and Salk, M., "Analysis of gravity anomalies with hyperbolic density contrast: An application to the gravity data of Western Anatolia," *Journal of the Balkan Geophysical Society*, **5**, pp. 87-96 (2002).
22. Biot, M. A., *Mechanics of Incremental Deformation*, John Willey and Sons, New York (1965).
23. Biot, M. A., "Non-linear theory of elasticity and the linearized case for a body under initial stress," *The London, Edinburgh, and Dublin Philosophical Magazine and Journal of Science*, **27**, pp. 468-489 (1939).
24. Chattopadhyay, A. *et al.*, "Torsional surface waves in heterogeneous anisotropic half-space under initial

https://doi.org/10.1017/jmech.2017.1 Published online by Cambridge University Press

stress," *Archive of Applied Mechanics*, **83**, pp. 357-366 (2013).

25. Samal, S. and Chattaraj R., "Surface wave propagation in fiber-reinforced anisotropic elastic layer between liquid saturated porous half space and uniform liquid layer," *Acta Geophysica*, **59**, pp. 470-482 (2011).
26. Tierstein, H. F., *Linear Piezoelectric Plate Vibrations*, Plenum Press, New York, (1969).

(Manuscript received February 19, 2016,
accepted for publication December 6, 2016.)

https://doi.org/10.1017/jmech.2017.1 Published online by Cambridge University Press

https://doi.org/10.1017/jmech.2017.1 Published online by Cambridge University Press